Konya Mühendislik Bilimleri Dergisi, c. 13, s. 2, 489-509, 2025
Konya Journal of Engineering Sciences, v. 13, n. 2, 489-509, 2025
ISSN: 2667-8055 (Electronic)
DOI: 10.36306/konjes.1585863

EFFECT OF GRAPHITE AND MAX PHASE ON THE THERMAL AND DIELECTRIC PROPERTIES OF N-VINYL CARBAZOLE AND BENZYL METHACRYLATE COPOLYMER

[1,*] Esra BARIM, [2] Emrah GUNDOGDU

[1] *Munzur University, Vocational School of Tunceli, Tunceli, TÜRKİYE*
[2] *Munzur University, Munzur University Institute of Sciences, Tunceli, TÜRKİYE*
[1]esrabarim@munzur.edu.tr, [2]emrahgundogdu62@gmail.com

Highlights

- A copolymer containing NVC and BZMA monomers was synthesized and its composites with graphite/Ti_3AlC_2 (MAX phase) were made and characterized.
- The effects of graphite/MAX phase on the thermal and electrical behaviour of the copolymer were investigated.
- The glass transition temperature of the copolymer increased in direct proportion to the doped graphite/MAX phase content.
- .Two of the composites were evidenced to be semiconductors by their electrical behaviour.
- The dielectric performance of copolymer was improved with graphite/MAX phase for use as functional components in energy storage devices

Graphical Abtract

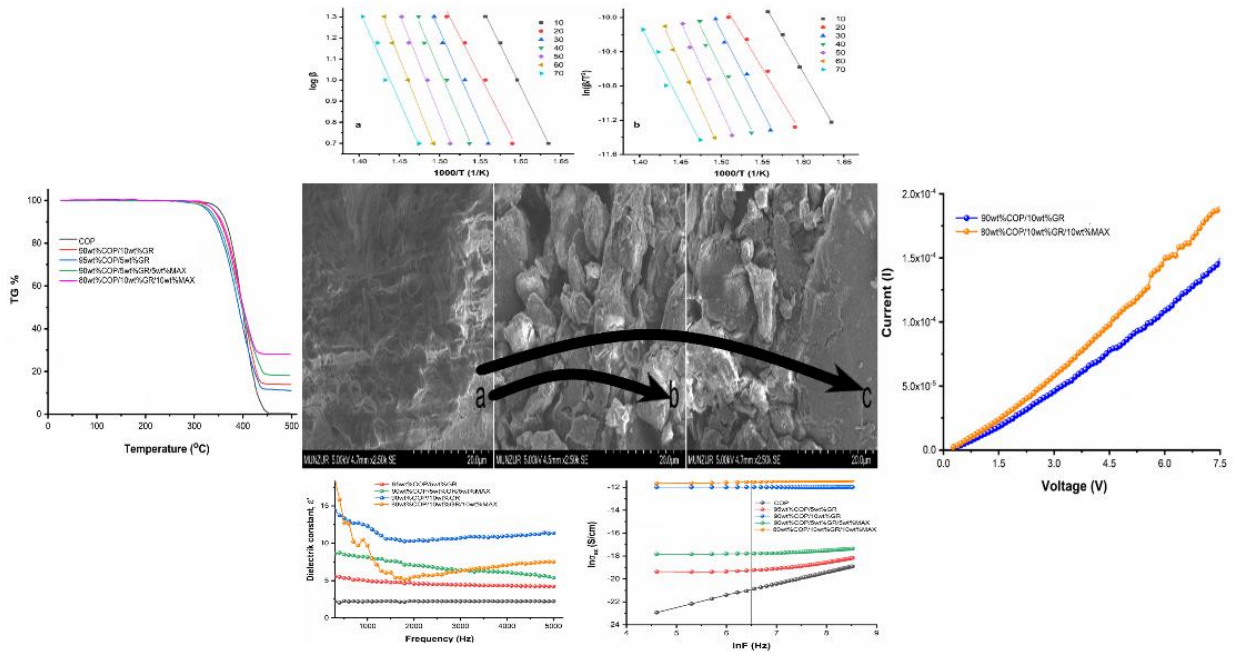

***Corresponding Author:** Esra BARIM, esrabarim@munzur.edu.tr

Konya Mühendislik Bilimleri Dergisi, c. 13, s. 2, 489-509, 2025
Konya Journal of Engineering Sciences, v. 13, n. 2, 489-509, 2025
ISSN: 2667-8055 (Electronic)
DOI: 10.36306/konjes.1585863

EFFECT OF GRAPHITE AND MAX PHASE ON THE THERMAL AND DIELECTRIC PROPERTIES OF N-VINYL CARBAZOLE AND BENZYL METHACRYLATE COPOLYMER

[1,*] Esra BARIM, [2] Emrah GUNDOGDU

[1] *Munzur University, Vocational School of Tunceli, Tunceli, TÜRKİYE*
[2] *Munzur University, Munzur University Institute of Sciences, Tunceli, TÜRKİYE*
[1]esrabarim@munzur.edu.tr, [2]emrahgundogdu62@gmail.com

(Received: 15.11.2024; Accepted in Revised Form: 09.04.2025)

ABSTRACT: In this study, the P(N-vinyl carbazole-co-benzyl methacrylate) copolymer was synthesized, characterized by FT-IR/^{1}H-NMR spectroscopic methods, and its composition was calculated from ^{1}H NMR spectra. Composites of the copolymer with four different ratios of graphite (GR) and MAX phase (Ti_3AlC_2) by weight were prepared to obtain functional and novel electronic components for energy storage applications. Scanning electron microscopy, X-ray diffraction analyses were performed for some samples. Differential scanning calorimetry, thermogravimetric analysis curves were used to determine the thermal behavior of the materials. It was concluded that the composite with the highest glass transition temperatures and thermal stability was the composite with 10wt%GR/10wt%MAX additive. The thermal degradation kinetics of the copolymer and the composite containing 10wt%GR/10wt%MAX were investigated by applying the Flynn-Wall-Ozawa (FWO), Kissinger-Akahira-Sunose (KAS) methods and it was found that the thermal degradation activation energy of the composite was lower than that of the polymer. The dielectric properties of the materials were investigated at room temperature and between 0.1 kHz and 5 kHz. At 1 kHz the dielectric constants of the copolymer and 10wt%GR-doped composite were found to be 2.22 and 12.31, respectively. The composites doped with 10wt%GR and 10wt%GR/10wt%MAX were confirmed to be semiconductors.

Keywords: *N-Vinylcarbazole, Benzyl Methacrylate, Graphite, MAX, Composite, Activation Energy, Dielectric*

1. INTRODUCTION

Polymers, as cornerstones of materials science, have facilitated innovations that touch every aspect of our lives at all times. The use of polymers in combination with other organic and inorganic materials to improve the properties of the materials has led to the growth of composite studies. Composite materials are the focus of much scientific research due to their outstanding properties such as thermal resistance and conductivity [1-3]. Polymer composites are materials consisting of a polymer matrix reinforced with other materials known as fillers or reinforcing materials. The polymer matrix provides a stable structure, while the reinforcements offer specific mechanical, thermal, or electrical properties. These composites have found applications in optoelectronic devices, energy storage applications, the chemical industry, and many other sectors [4-8].

N-vinyl carbazole (NVC) and benzyl methacrylate (BZMA) monomers are frequently used in copolymerization and composite studies due to their unique properties. NVC, valued for its molecular ordering, is a significant monomer in materials science. It enables the synthesis of novel and functional polymers through addition polymerization with compatible monomers. The carbazole ring in the structure of NVC promotes π-conjugation within the polymer, enhancing its optical and electronic properties. P(NVC), the polymer derived from this monomer, has broad applications in organic solar cells, coatings, lenses, sensors, photovoltaic devices, and electroluminescent devices within the polymer industry as a result of its photophysical properties [9, 10]. Despite its widespread use, P(NVC) has limitations that affect its suitability for certain applications. Its low dielectric constant of approximately 3 [11-13] restricts its potential in energy storage applications, while its high glass transition temperature (Tg) of about 227 °C [14] limits its processability. These characteristics are significant drawbacks preventing

Corresponding Author: Esra BARIM, esrabarim@munzur.edu.tr

P(NVC) from broader use as a polymeric material [11, 14]. The dielectric properties of materials can be suitable for some applications and limiting for others. For example, In general materials with low dielectric constants are used for electronic packaging systems and materials with high dielectric constants are used for energy storage devices [15, 16]. The dielectric properties strongly depend on ambient properties such as temperature, frequency, etc., as well as the percentage of the composition of the copolymer [17]. To address these limitations of P(NVC), which is notable for its thermal stability and optical and dielectric properties [18, 19], researchers have explored various copolymers and composites. For example, Bilbao et al. synthesized NVC copolymers with different acrylate and methacrylate monomers [20], Haldar et al. developed P(NVC)/$Fe3O_4$ composites [21], Sonone et al. investigated P(NVC)/TiO_2 composite films [22], and Goumri et al. studied P(NVC)/graphene oxide composites [23]. Recently, Muntaser et al. reported that P(NVC)/polyvinyl chloride (PVC)/ZnO nanocomposite films exhibited enhanced thermal stability and dielectric-conductivity properties [24]. Duran et al. examined P(NVC)/TiO_2 composites and reported their suitability as corrosion-resistant coating materials [25]. Research on P(NVC) is ongoing [26-28]. The BZMA monomer is a methacrylic monomer containing a phenyl group in its structure. Although widely applied in various fields [29-32], BZMA has primarily been used in copolymerization studies to impart thermal functionality [33]. For instance, Xie et al. synthesized copolymers with varying BZMA and MMA compositions in microsphere form, highlighting that properties such as thermal stability and glass transition temperature (Tg) can be adjusted based on the monomer's composition [29]. Demirelli et al. reported that the dielectric constant of P(BZMA) was 3.22, with a Tg of 73 °C at 1 kHz at room temperature. They prepared composites of BZMA with lactone end groups and graphene, observing that the composite's thermal stability increased while Tg decreased in parallel with the amount of graphene added [33, 34].

Graphite (GR), a widely preferred reinforcement material in recent polymer composite studies, is an allotrope of carbon known for its excellent electrical conductivity due to delocalized electrons within its structure. Graphite's durability in terms of thermal properties also makes it suitable for various industrial applications [35]. Consequently, it is often chosen in composite studies to enhance the dielectric, electrical, and thermal properties of materials [36-38]. Another reinforcement material gaining popularity in recent years is the MAX phase. The MAX phase is a three-layered compound with the general formula $M_{n+1}AX_n$, where M is a transition metal, A is a group A element, X is carbon or nitrogen, and n ranges from 1 to 3. MAX phases are named based on the value of n; for example, Ti_3AlC_2 is referred to as a 312 MAX phase [39]. MAX phases are ideal for various structural applications in industry due to their resistance to high temperatures and corrosion. Additionally, their metallic conductivity makes them suitable for electrical contacts, sensors, and electronic devices [40-44].

This study aimed to develop functional semiconducting polymer composite systems with enhanced thermal stability, processability, and specific dielectric and electrical properties suitable for energy storage applications in various devices. For this purpose, a copolymer was synthesized from NVC-BZMA monomers. Composites of this polymer with reinforcement materials, namely GR and/or a MAX phase (Ti_3AlC_2), were prepared in four different weight ratios. The thermal, dielectric, and electrical properties of the polymer and its composites were then investigated. The results indicated that the reinforcing materials had a substantial thermal impact on the polymer system and significantly improved its dielectric and electrical properties.

2. MATERIALS AND METHODS

The monomers used for copolymer synthesis were N-vinyl carbazole (193.244 g/mol) and benzyl methacrylate (176 g/mol), with azobisisobutyronitrile (AIBN) as the initiator for the polymerization reaction. All reagents were obtained from Sigma-Aldrich. N-vinyl carbazole was purified by crystallization in methanol and used. Benzyl methacrylate was purified by washing with sodium hydroxide, and AIBN was purified by crystallization in chloroform. Analytically pure solvents including 1,4-dioxane (Sigma-Aldrich), dichloromethane (Merck), and ethyl alcohol (Sigma-Aldrich) were used in the study. Nitrogen gas was introduced during the polymerization reaction to eliminate oxygen radicals,

while graphite (GR; <20 μm Sigma Aldrich) and the MAX phase (Ti_3AlC_2; ≤100 μm particle size, Sigma-Aldrich) were used as reinforcement materials in the composite preparation stage. For sonication during composite preparation, an FY-US-01 FYtronix digital ultrasonic homogenizer was employed. Fourier transform infrared (FT-IR) spectra were obtained using a PerkinElmer Spectrum 100 model FT-IR spectrophotometer and ^{1}H NMR spectra was recorded on a Bruker Avance 300 MHz NMR instrument in $CDCl_3$ solvent. X-ray diffraction (XRD) data were acquired in the range of 10–90° at 2θ using a Rigaku Miniflex600 X-ray diffractometer device and scanning electron microscopy (SEM) images were captured with a Hitachi SU3500 device. TGA curves for the copolymer and composites were obtained by heating from room temperature to 500 °C in aluminum containers at a rate of 10 °C/min in a nitrogen gas atmosphere using a Shimadzu TGA-50 device. DSC analysis of the polymer and composites was conducted using a Shimadzu DSC-60A device in the range of 25 °C to 250 °C. For dielectric measurements, a QuadTech 7600 LRC impedance analyzer was used.

2.1. Synthesis of the Copolymer

The P(N-vinyl carbazole-co-benzyl methacrylate) copolymer was synthesized via the free radical polymerization method. 6 mmol NVC and 4 mmol BZMA monomers were placed in a polymerization tube together with AIBN at a rate of 1% of the total weight of the monomers, dissolved in 1,4-dioxane solvent. The solution in the polymer tube was passed through nitrogen gas for five minutes and then the cap was closed. The polymerization reaction was conducted in an oil bath at 70 °C for 12 hours. Ethyl alcohol was used to precipitate the resulting polymer and this process was repeated three times to ensure complete removal of any residual monomer. The final product was obtained as a white solid. The P(N-vinyl carbazole-co-benzyl methacrylate) copolymer, designated as COP, was then dried in a vacuum oven at 40 °C for 24 hours. FT-IR and ^{1}H NMR spectroscopy were used for structural characterization. The synthesis scheme of the copolymer is shown in Figure 1.

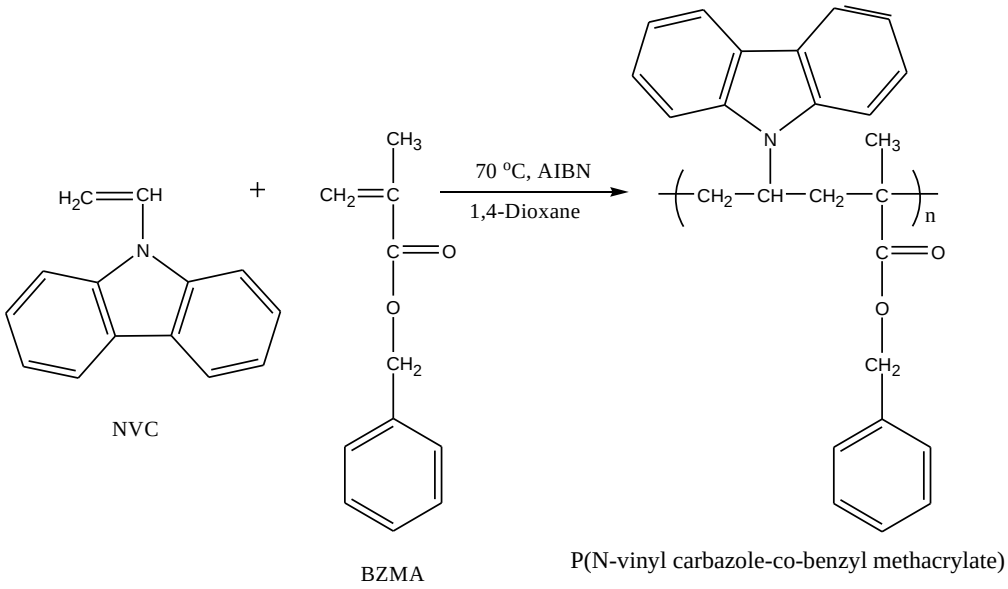

Figure 1. Synthesis scheme of P(N-vinyl carbazole-co-benzyl methacrylate) (COP) copolymer

2.2. Preparation of COP/Graphite/MAX Composites

All composites were prepared by the solvent casting method in three steps using dichloromethane as the solvent. COP was used as the polymer matrix, while graphite (GR) and MAX (Ti_3AlC_2) served as the reinforcement materials. In the first step, the specified amount of copolymer was dissolved in a beaker

containing solvent. In the second step, the reinforcement material, weighed at a specific ratio relative to the polymer matrix, was dispersed in a separate beaker with solvent for 1 hour. In the final step, the dispersed reinforcement material was added to the polymer solution, and the solvent was removed using an evaporator. The resulting composite materials were first air-dried and then placed in a vacuum oven at 40 °C until they reached a constant weight. The composites were designated as 95wt%COP/5wt%GR, 90wt%COP/10wt%GR, 90wt%COP/5wt%GR/5wt%MAX, and 80wt%COP/10wt% GR/10wt% MAX. This nomenclature is based on the amount of material used by weight when preparing the composites. For example, the first sample was prepared using 95 mg copolymer and 5 mg graphite.

3. FINDINGS AND DISCUSSION

3.1. FT-IR analysis

In the FT-IR spectrum of the COP polymer shown in Figure 2, peaks at 3032 and 3064 cm^{-1} correspond to aromatic C-H stretching vibrations, while peaks at 2937–2978 cm^{-1} correspond to aliphatic C-H stretching vibrations. The 1721 cm^{-1} peak indicates the ester carbonyl group, the 1450 cm^{-1} peak is associated with C=C stretching vibrations in the aromatic ring, the 1331 cm^{-1} peak is attributed to vinylidene, and the 1158–1220 cm^{-1} peaks correspond to the (-C=O)-O-C group. The 694 cm^{-1} peak is attributed to C-H stretching vibrations of monosubstituted benzene rings [45-47]. No functional groups related to graphite were observed in the FT-IR spectrum [48]. Additionally, the absence of a peak around 1635 cm^{-1} corresponding to the CH_2=CH- structure from the monomers confirms the formation of the copolymer. The FT-IR spectra of the composites exhibit all the peaks observed in the copolymer spectrum. However, in the composite spectra, the copolymer peaks show a shift to lower wave numbers and are broadened due to the influence of the reinforcing materials. This may be due to the interactions between the polymer matrix and the reinforcing material graphite. This shift indicates successful doping of the composite [36, 49, 50].

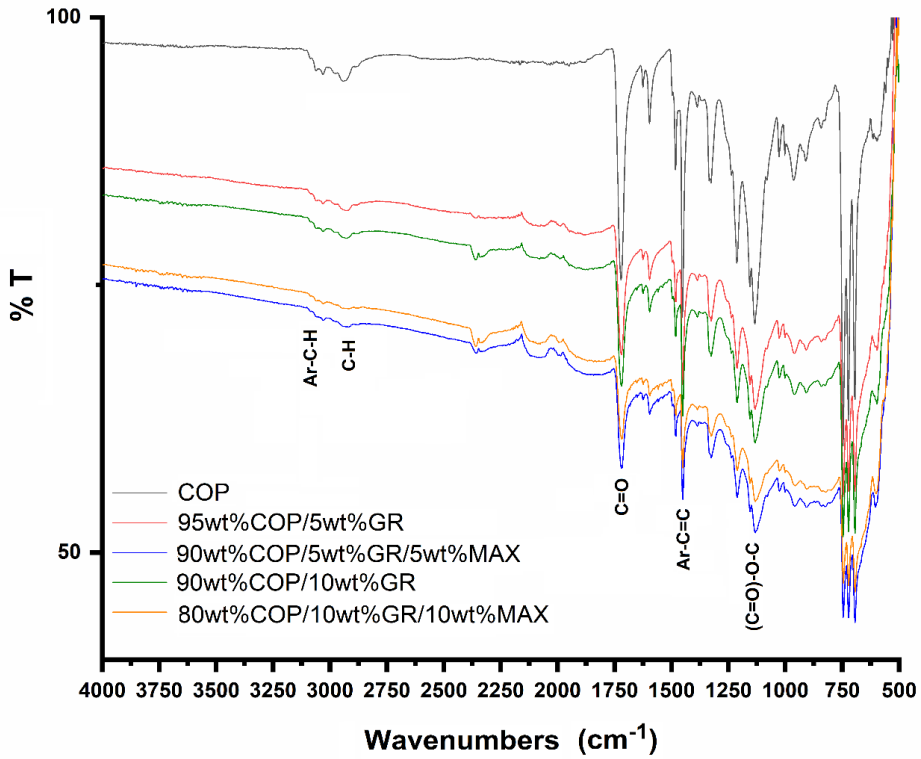

Figure 2. FT-IR spectrum of COP and its composites

3.2. ^{1}H NMR analysis and composition determination of the COP copolymer

In the ^{1}H NMR spectrum of the copolymer shown in Figure 3, the peaks between 0.3 and 1.6 ppm correspond to the -CH_3 and -CH_2 protons in the polymer chain, the peak at 4.8 ppm represents the -O-CH_2 protons of the BZMA monomer, and the peaks between 6.5 and 8 ppm indicate protons associated with the aromatic rings of the NVC and BZMA monomers [45]. The presence of signals characteristic of the copolymer structure and the absence of signals for vinylic protons at 6.5 and 5.5 ppm confirm the successful synthesis of the copolymer.

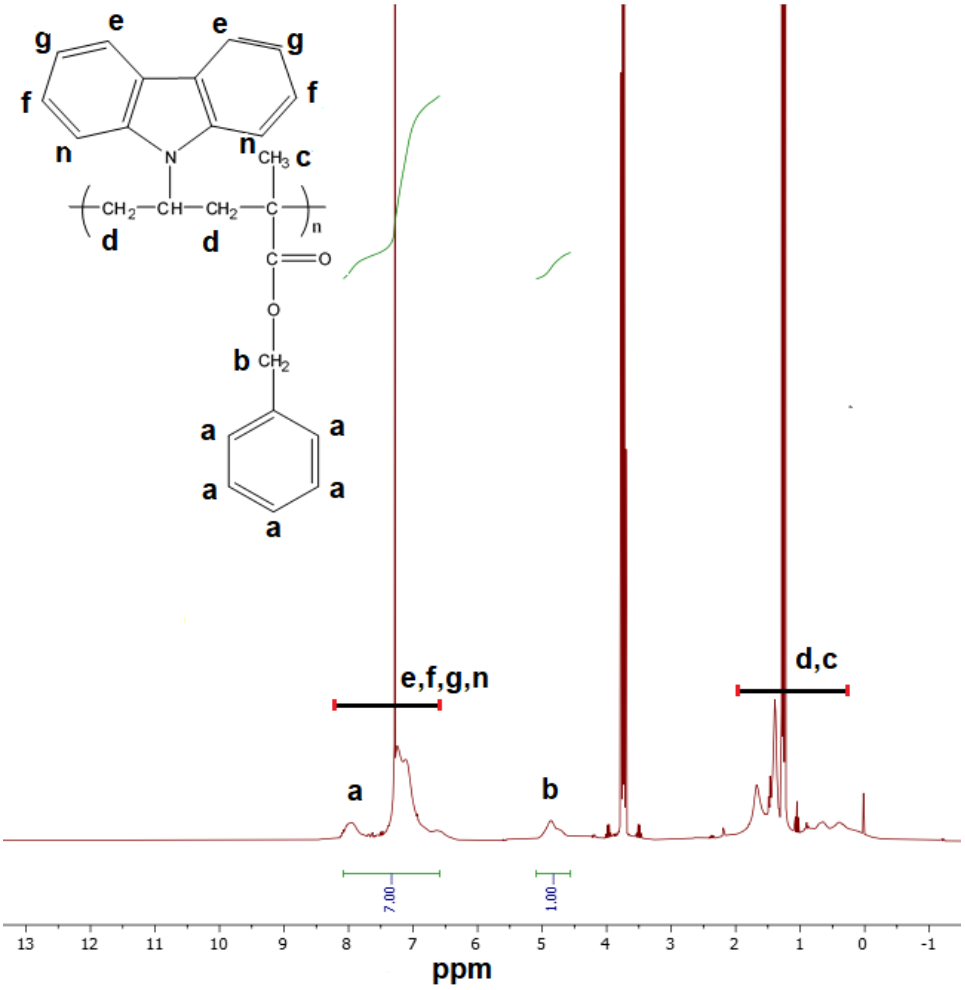

Figure 3. ^{1}H NMR spectrum of COP polymer

The percentage composition of the copolymer was determined based on the ^{1}H NMR spectrum. Integral heights of the aromatic ring protons of the NVC and BZMA units, as well as the O-CH_2 protons of the BZMA units in the copolymer, were used in the calculation. Equations 1 and 2 were applied to calculate the copolymer composition.

$$\frac{Integral\ height\ of\ aromatic\ protons}{Integral\ height\ of\ OCH_2\ protons} = \frac{8m_1 + 5m_2}{2m_2} = \frac{7}{1} \quad (1)$$

$$m_1 + m_2 = 1 \quad (2)$$

Here, m_1 is the mole fraction of NVC units in the copolymer and m_2 is the mole fraction of BZMA units. According to the calculations, the composition of the COP copolymer consisted of 53% NVC units and 47% BZMA units.

3.3. XRD analysis

XRD analyses of the 90wt%COP/10wt%GR and 80wt%COP/10wt%GR/10wt%MAX composites shown in Figure 4. In the spectrum of the 90wt%COP/10wt%GR composite in Figure 4a, graphite (Card number, 9011577) produced a signal at 2θ = 54.45° (001) with the strongest signal at 2θ = 26.5° (002) [51]. Figure 4b displays the XRD spectrum of the 80wt%COP/10wt%GR/10wt%MAX composite, with signals observed at 2θ = 9.50° (002), 19.08° (004), 26.5°(002), 33.9° (101), 36.6° (103), 38.9° (104), 41.6° (105), 54.7° (004), 60.04° (110), 65.32° (1011), 73.76° (118). At 26.5° the signal correspond to graphite (Card number, 9012230), while the MAX phase (Card number 7221324) gives its most characteristic signal at 38.9° [52, 53]. The broad signal in the range of 19.08° to 28.79° is due to the amorphous structure of the polymer [54].

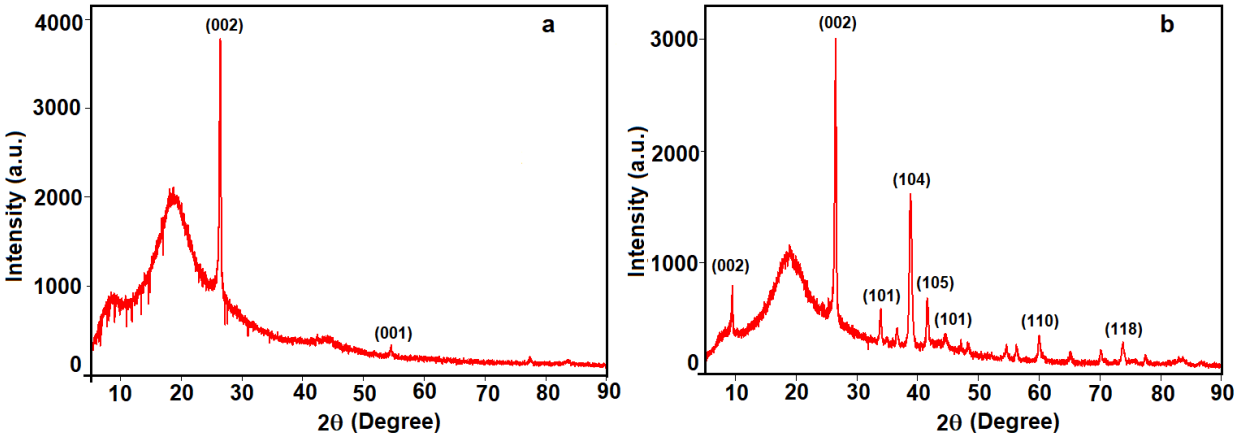

Figure 4. XRD spectra of a) 90wt%COP/10wt%GR b) 80wt%COP/10wt%GR/10wt%MAX

3.4. SEM analysis

SEM images of the surface morphologys of pure polymer and some of its composites of the surface morphologys were showed in Figure 5. It was observed that the copolymer, which initially exhibited a surface that appeared as if it had pores, lost this appearance after doping and generally turned into a rough, tightly packed structure [52]. Comparing the surface morphologies of the composites with the SEM images of the copolymer reveals significant changes, indicating successful doping.

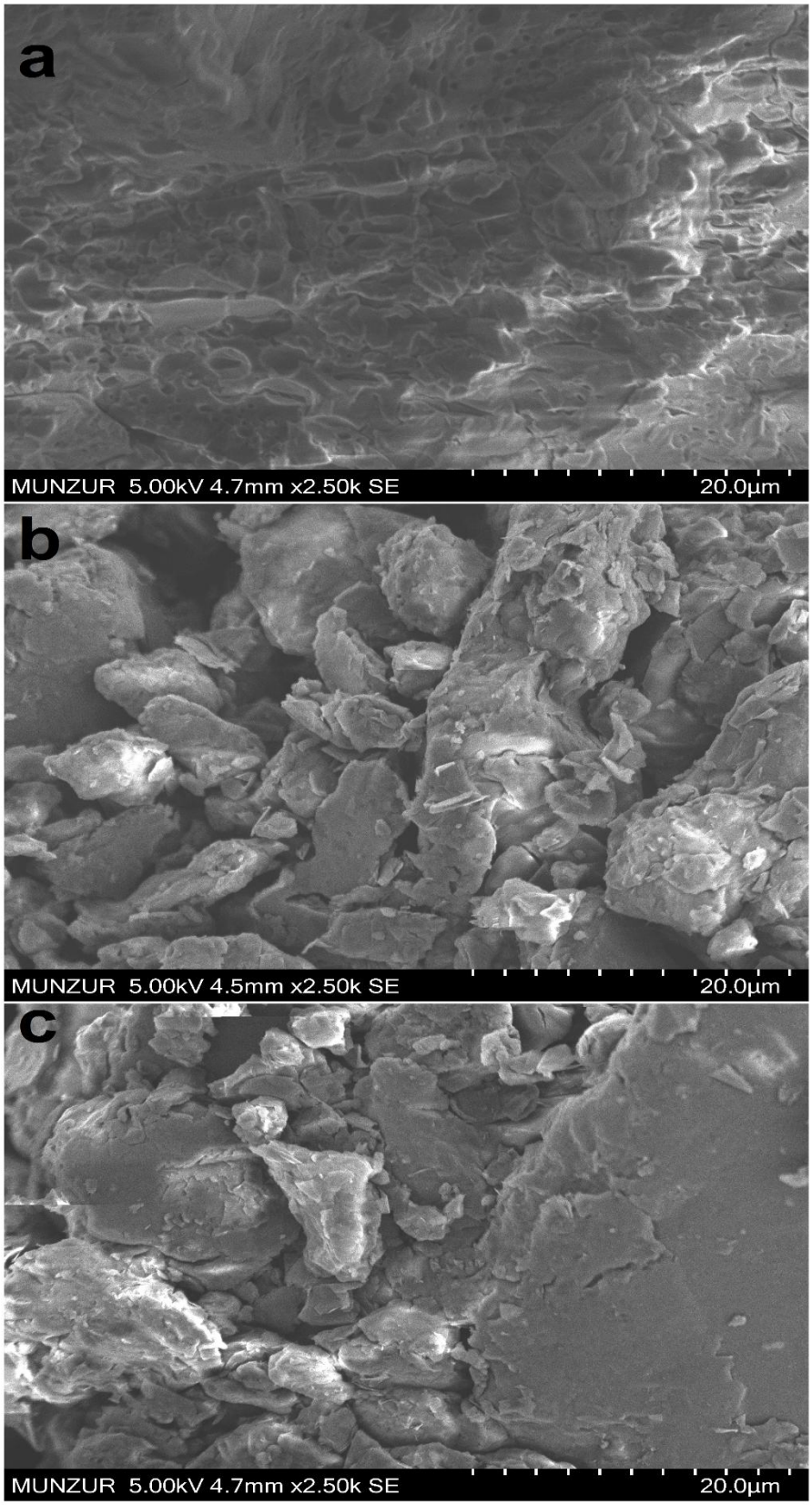

Figure 5. SEM micrographs of a) COP, b) 90wt%PCOP/10wt%GR, and c) 80wt%COP/10wt%GR/10wt%MAX

3.5. Thermal Analysis

3.5.1. DSC analysis

DSC analysis of the polymer and composites shown in Figure 6. Glass transition temperatures (Tg) are provided in Table 1. The Tg values of the polymer and composites whose DSC curves are displayed in Figure 6 fall within the Tg range of P(NVC) (227 °C) and P(BZMA) homopolymers (73 °C). The Tg value of COP polymer is 101.74 °C. It was observed that the Tg values of the composites increased by approximately 2 °C compared to the polymer alone. These increases in Tg were noted to occur with progressively higher concentrations of GR and/or MAX. While 5 wt%GR doping raised the Tg value of the polymer by 0.37 °C, both GR and MAX phase doping resulted in an increase exceeding 1.7 °C. Changes in Tg values in amorphous polymers are associated with the mobility or flexibility of polymer chains [55]. The higher Tg values observed in composites compared to polymer are attributed to the influence of reinforcement materials on the polymer chain. This effect is due to the reinforcement materials restricting polymer chain mobility, thereby reducing the polymer's free volume and raising the glass transition temperatures [56].

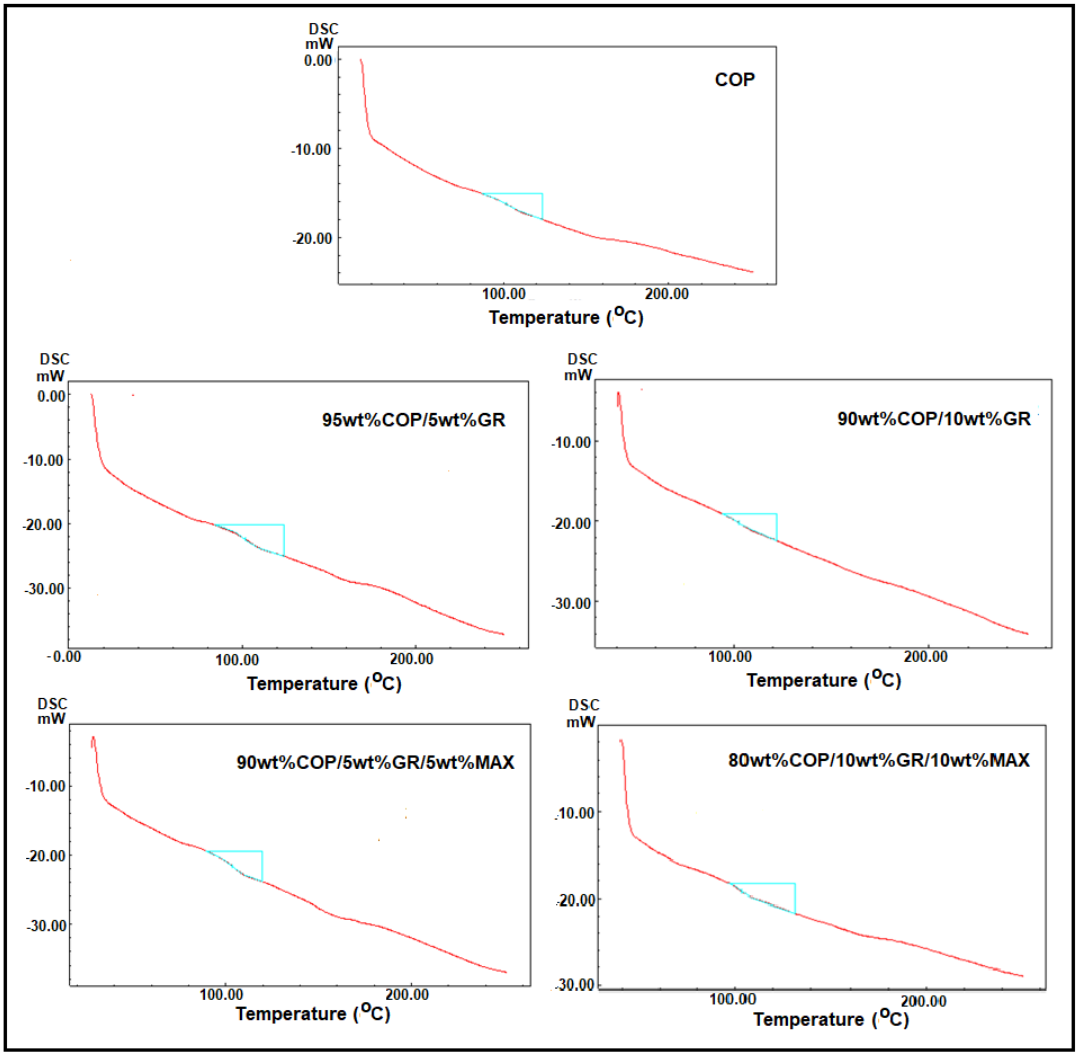

Figure 6. DSC curves of COP and composites

Table 1. Tg values of polymer and composites

Polymers and composites	Tg (°C)
COP	101.74
95wt%COP/5wt%GR	102.11
90wt%COP/10wt%GR	102.72
90wt%COP/5wt%GR/5wt%MAX	103.50
80wt%COP/10wt%GR/10wt%MAX	103.70

3.5.2. TGA analysis

TGA curves for the copolymer and composites shown in Figure 7. Thermal data calculated from the TGA thermograms are presented in Table 2. The initial decomposition temperature of the copolymer was 330 °C, while it decreased across all composites. Adding 5wt%GR to the polymer reduced the initial decomposition temperature by 39 °C, and the inclusion of 10wt%GR and 10wt%MAX lowered it by 12 °C. Generally, to assess the thermal stability of polymeric materials, temperature values indicating 50% weight loss are examined [57]. Doping of 10wt%GR and 10wt%GR/10wt%MAX improved the thermal stability of the polymer by 0.5 °C and 3 °C, respectively. These increases may have resulted from strong interfacial interactions of GR and MAX with the polymer matrix [58]. The composite with the highest thermal stability (401.5 °C) was the one doped with 10wt%GR and 10wt%MAX. Furthermore, the residue content of the composites increased with higher amounts of GR and MAX, both of which are highly resistant to heat, indicating that the composite with the highest GR and MAX content also had the greatest residual weight.

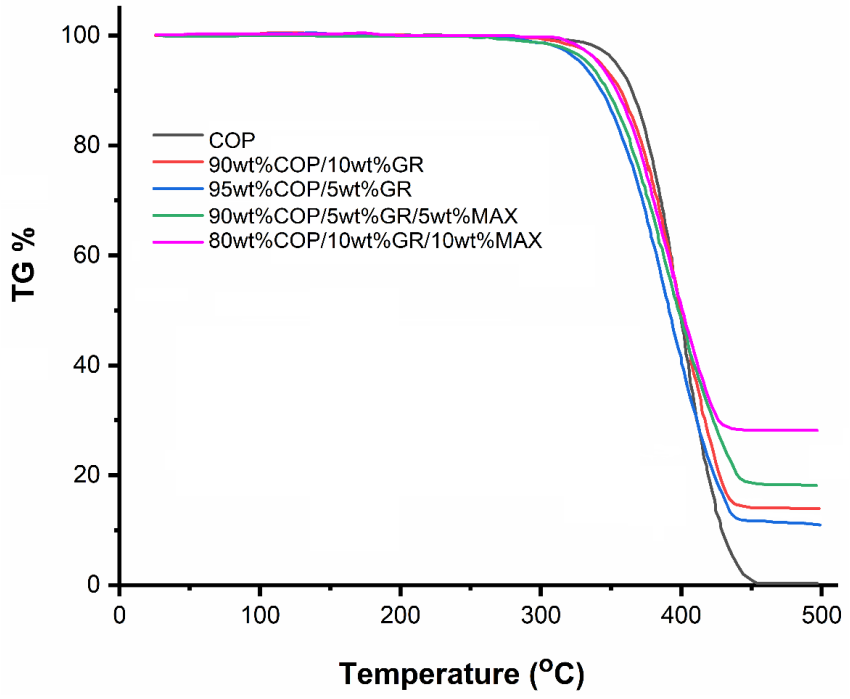

Figure 7. TGA curves of polymer and composites at 10 °C/min

Table 2. Thermal data of polymer and composites at 10 °C/min heating rate

Polymer and Composites	T_{int} (°C)	%10	%30	%50	%70	%90	% Residue at 500 °C
COP	330	365.0	386.0	398.5	411.0	424.0	-
95wt%COP/5wt%GR	291	343.5	372.0	390.5	411.0	-	11.56
90wt%COP/10wt%GR	307	357.0	383.0	399.0	418.0	-	13.76
90wt%COP/5wt%GR/5wt%MAX	293	347.0	377.0	397.5	422.5	-	17.88
80wt%COP/10wt%GR/10wt%MAX	318	354.5	380.0	401.5	427.0	-	27.6

T_{int}: Initial decomposition temperature

3.5.3. Thermal Degradation Kinetics of COP and 80wt%COP/10wt%GR/10wt%MAX

Thermal degradation kinetic data for polymers are essential parameters that aid in understanding the thermal degradation process of these materials. One commonly used method for investigating polymer thermal degradation kinetics is calculating thermal degradation activation energies by analyzing thermogravimetric analysis (TGA) data. Thermal decomposition is closely related to the heating rate, with characteristic temperature points changing in TGA curves taken at different heating rates for the same material [59, 60].

All kinetic studies operate under the assumption that the isothermal rate of conversion, $d\alpha/dt$, is a linear function of k (T) (the temperature-dependent rate constant) and $f(\alpha)$ (a function of the non-temperature-dependent conversion), as shown in Equation 3 [61, 62].

$$\frac{d\alpha}{dt} = \beta \frac{d\alpha}{dt} = k(T) f(\alpha) \tag{3}$$

$$\alpha = \frac{m_0 - m_t}{m_0 - mf} \tag{4}$$

In these equations, m_o represents the initial mass of the sample, m_t is the instantaneous mass, and m_f is the final mass. α denotes the degree of transformation, which is determined from TGA data. t is the time and T is the temperature. The constant heating rate is denoted by β (where $\beta = dT/dt$) and k (T) is the rate constant. The result is expressed with the Arrhenius equation, as shown in Equation 5.

$$k(T) = Ae^{-E_a/RT} \tag{5}$$

In Equation 5, A is the exponential factor (K^{-1}), E_a is the activation energy (kJ/mol), T is the absolute temperature (°C), and R is the universal gas constant (R = 8.314 J/mol K). When these equations are combined, Equation 6 can be written [63].

$$\frac{d\alpha}{dt} = Ae^{-E_a/RT} f(\alpha) \tag{6}$$

Some kinetic methods recommended by the International Confederation for Thermal Analysis and Calorimetry (ICTAC) are available in the literature [64]. Among these, the Flynn-Wall-Ozawa (FWO) and Kissinger-Akahira-Sunose (KAS) models are frequently used to calculate the activation energy of polymer thermal degradation [50]. Both methods are integral methods that are independent of reaction order. In the FWO method, parallel curves are obtained by plotting log β against 1000/T at varying heating rates. E_a is calculated by determining the slope of these curves. Equation 7 is used for the FWO method [65, 66].

$$log(\beta) = log\left[\frac{AEa}{g(a)R}\right] - 2.315 - \frac{0.457\,Ea}{RT} \tag{7}$$

In the above equation, (α) is an unknown function of the conversion. According to this equation, the activation energy (–0.457 E_a/RT) is calculated using the slope of the log $\beta^{-1}/T(K^{-1})$ plot.

When applying the KAS method to calculate the activation energy, ln (β/T^2) is plotted against $1/T(K^{-1})$. The value of E_a is calculated from the slope of the linear lines obtained from this graph. The equation for the KAS method is defined in Equation 8 [67].

$$ln\left(\frac{\beta}{T^2}\right) = ln\left(\frac{AR}{g(\alpha)Ea}\right) - \frac{Ea}{RT} \quad (8)$$

In this context, to calculate the E_a values, TGA thermograms of the polymer and its composite containing 10 wt.% GR/10 wt.% MAX were recorded with heating from 30 °C to 500 °C under a nitrogen atmosphere at heating rates of 5, 10, 15, and 20 °C/min, as shown in Figures 8a and 8b. The graphs for COP, where the FWO and KAS methods were applied, are presented in Figures 9a and 9b.

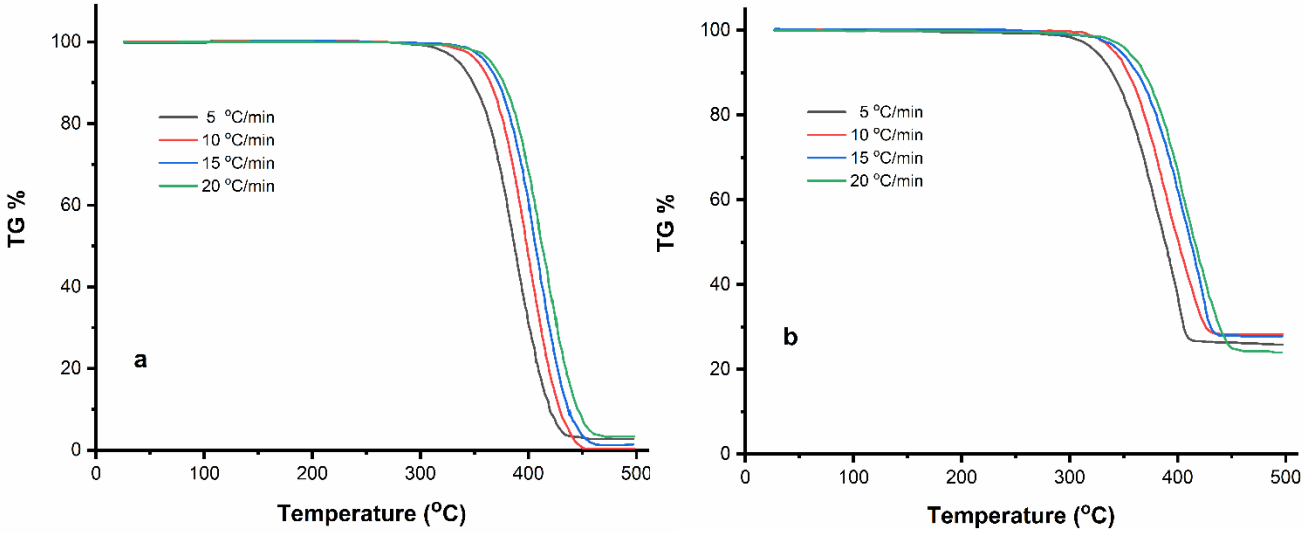

Figure 8. TGA curves of (a) polymer and (b) composite at different heating rates

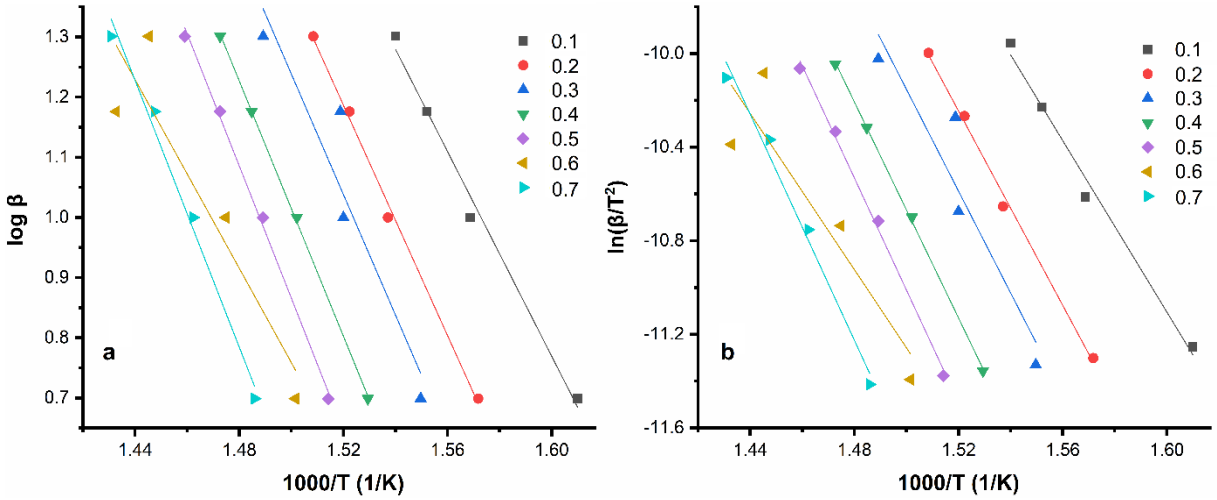

Figure 9. Kinetic curves of thermal degradation of copolymer at different conversion rates: (a) FWO method, (b) KAS method

To understand the effect of doping materials GR and MAX on the polymer's degradation process, the thermal degradation activation energy of the composite containing 10wt%GR/10wt%MAX was analyzed,

with the activation energy determined in the same way as for the copolymer. The composite's graphs according to the FWO and KAS methods are shown in Figures 10a and 10b.

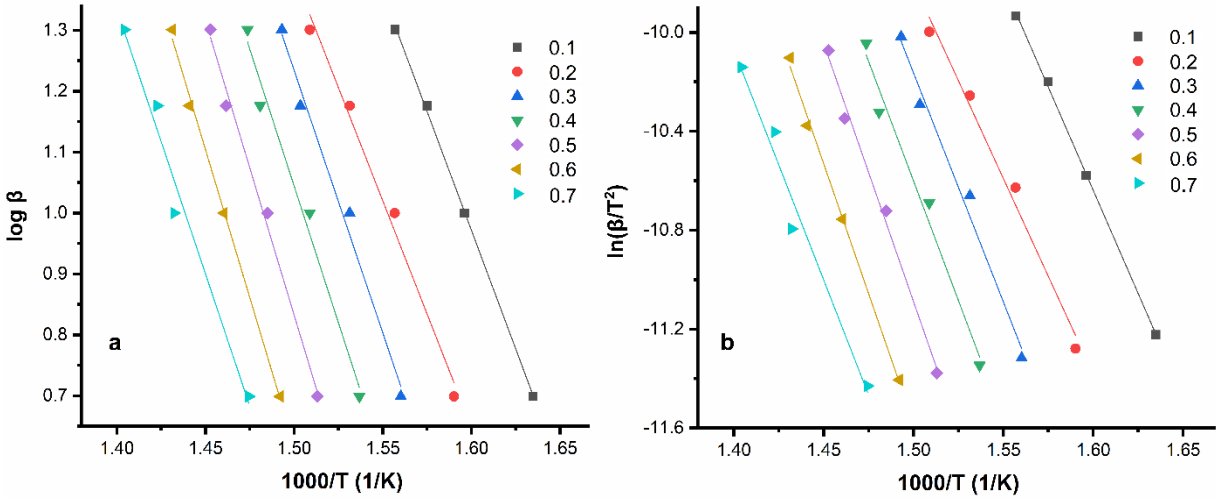

Figure 10. Kinetic curves of thermal degradation of 80wt%COP/10wt%GR/10wt%MAX composite at different conversion rates: (a) FWO method, (b) KAS method

The thermal degradation activation energies of the polymer and its composite, calculated from the FWO and KAS graphs for conversions from 0.1 to 0.7, are presented in Table 3. As shown in Table 3, the activation energy of the polymer increased from 0.1 to 0.6, decreased at 0.6, and then increased again at 0.7. The lines are nearly parallel across all conversions, with the exception of the non-parallel line at 0.6, attributed to the complexity of the dissociation mechanism [63]. In the composite, the activation energy increased up to 0.7 before decreasing at this point. The increasing E_a values of the composite at conversions above 0.1 are due to the significant impact of GR and MAX on the polymer. The thermal degradation activation energies for the polymer were determined as 178.3 kJ/mol and 176.6 kJ/mol according to the FWO and KAS methods, respectively. For the composite, the values were 158.2 kJ/mol according to the FWO method and 155.5 kJ/mol according to the KAS method. In both systems, the E_a values were closest at a conversion value of 0.3. The composite's E_a values were lower than those of the polymer, indicating the notable effect of GR and MAX on the polymer's degradation process. The strong interfacial interactions between the reinforcing materials GR and MAX and the polymer matrix in the composite system increase the thermal stability of the polymer, as shown in Figure 6, while simultaneously accelerating the thermal degradation process. The growing tendency of the reinforcements to aggregate within the polymer matrix made the polymer susceptible to faster degradation.

Table 3. Thermal degradation activation energy values of COP and its composite calculated according to FWO and KAS methods

	COP		**Composites**	
Conversion (α)	**FWO Ea (kj/mol)**	**KAS Ea (kj/mol)**	**FWO Ea (kj/mol)**	**KAS Ea (kj/mol)**
0.1	154.7	152.3	141.7	138.7
0.2	174.2	172.1	135.1	131.5
0.3	182.2	180.8	156.7	154.0
0.4	192.9	191.9	163.4	160.9
0.5	199.9	199.7	175.7	173.7
0.6	142.6	138.7	176.8	174.7
0.7	201.6	200.8	158.0	154.7
Avarage	**178.3**	**176.6**	**158.2**	**155.5**

The average activation energy conversion plots for both the polymer and the composite are shown in Figures 11a and 11b, respectively. During the thermal degradation of the composite, activation energy increased with conversion. This rise in activation energy can be attributed to the barrier effect of the reinforcement materials, which protect the polymer as it undergoes thermal degradation at higher temperatures. As previously discussed, reinforcement materials GR and MAX play a substantial role in the thermal degradation stages of the polymer [68].

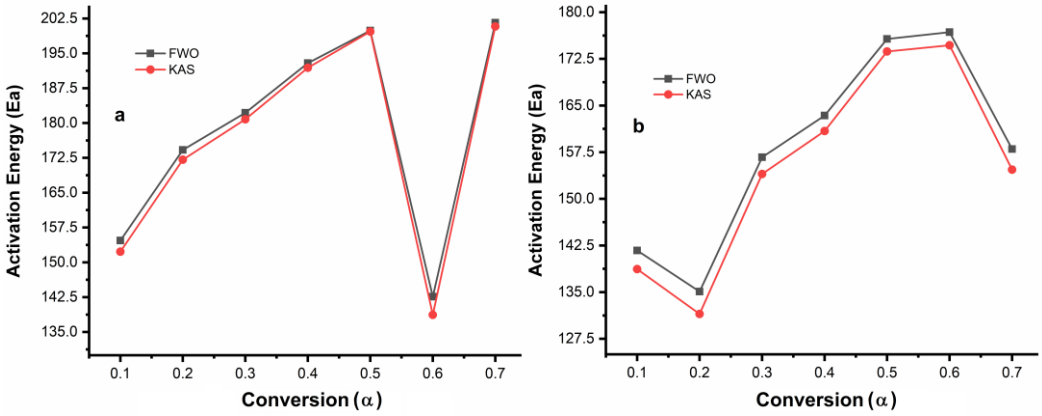

Figure 11. Activation energy conversion graph of a) COP and b) composite

3.6. Dielectric Measurements of Polymer and Composites

Dielectric measurements for the polymer and its composites were conducted at room temperature over a frequency range of 100 Hz to 5 kHz. Initially, pellets of the materials were prepared under four tons of pressure and their thickness was measured, and then dielectric measurements were performed. The dielectric constants of the materials were calculated from Equation 9 using capacitance (C_p).

$$\varepsilon^* = \varepsilon' + \varepsilon'' \tag{9}$$

In Equation 9, ε' represents the real part of the dielectric constant and ε'' is the imaginary part of the dielectric constant. The real part of the dielectric constant can be expressed by Equation 10.

$$\varepsilon' = \frac{C_p \cdot d}{\varepsilon_0 A} \tag{10}$$

Here, ε_o is the dielectric constant of the vacuum (8.854×10^{-12}), d is the thickness (m) and A is the surface area (m^2) of the sample, C_p is the parallel capacitance (F), and Df is the dielectric loss factor. For the imaginary part, Equation 11 can be written as follows [69, 70].

$$\varepsilon'' = \varepsilon' Df \tag{11}$$

The dielectric constant (ε')-frequency plot of the materials is presented in Figure 12 and the dielectric loss (ε'')-frequency plot is shown in Figure 13. The pure polymer exhibited a dielectric constant of 2.2 at 1 kHz at room temperature; however, the dielectric constant increased across all composites. The dielectric constants for 95wt%COP/5wt%GR, 90wt%COP/10wt%GR, 90wt%COP/5wt%GR/5wt%MAX, and 80wt%COP/10wt%GR/10wt%MAX composites were measured as 4.98, 12.31, 8.13, and 9.71, respectively. Among these, the smallest increase in the dielectric constant occurred with the addition of 5wt%GR, yet even this amount yielded a 2.26-fold increase. The dielectric constant increased 3.66-fold in the composite with 5wt%GR and 5wt%MAX and 4.41-fold in the composite containing 10wt%GR and 10wt%MAX. The composite with 10wt%GR achieved the highest dielectric constant at 12.31, marking the maximum increase observed. Additionally, while the dielectric loss of the pure polymer was –0.061 under identical

conditions, an increase was observed in all composites. Notably, composites containing 10% GR exhibited substantial increases in dielectric loss. The observed increases in dielectric properties suggest that the composites become highly polarized at low frequencies in alignment with the applied electric field. This can be attributed to charge accumulation at interfaces and interface polarization. As the concentration of reinforcing material in the composites rises, aggregation occurs, leading to greater polarization and elevated dielectric values. Additionally, both the dielectric constants and dielectric losses of the composites tend to decrease with increasing frequency. This reduction is due to the shorter time available for interface dipoles to orient in response to the alternating field, a common characteristic in conductor-insulator systems [71-73]. At higher frequencies, the almost constant values of ε′ and ε′′ reflect the reduced efficiency of orientation and interface polarization, which is generally more effective at low frequencies [74].

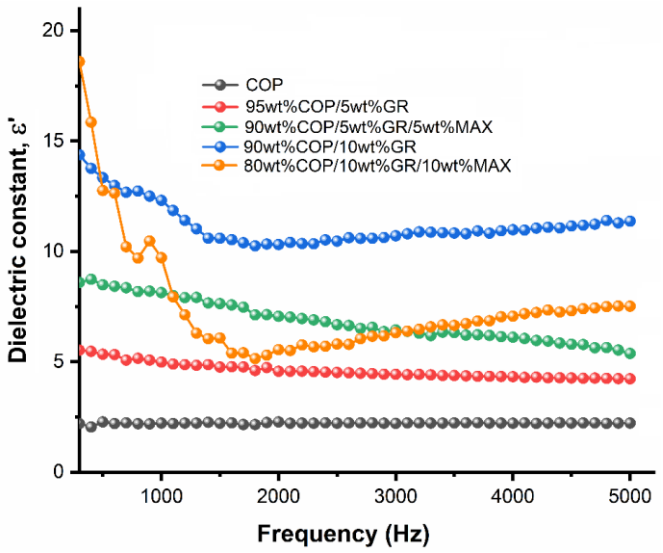

Figure 12. Plot of dielectric constants of COP and composites with frequency

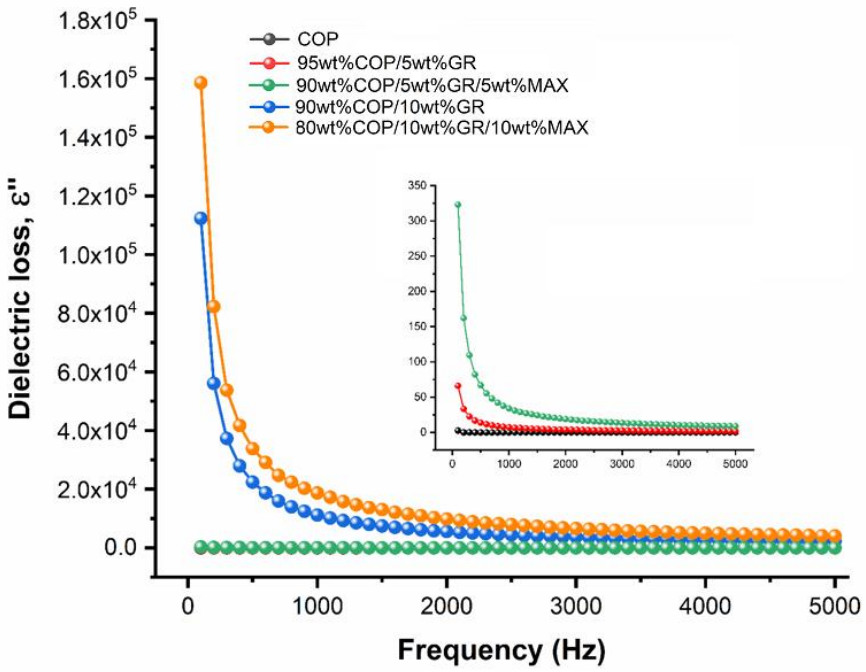

Figure 13. Variation of dielectric loss of COP and its composites with frequency

G_p (conductivity) values of polymer and composites were measured with an impedance analyzer device in the range of 100 Hz to 5 kHz. Conductivity (σ) (AC conductivity) values were calculated using Equation 12 [75].

$$\sigma = G_p \frac{d}{A} \tag{12}$$

When the conductivity-frequency plot given in Figure 14 is examined, it is observed that DC conductivity increases in composites compared to the pure polymer in Region I. GR and MAX, used as reinforcing materials in polymer composites, possess good semiconducting properties. The homogeneous distribution of these materials within the polymer matrix and the formation of a conductive path in the insulating matrix resulted in an increase in conductivity, particularly due to higher amounts of GR and MAX doping [75, 76].

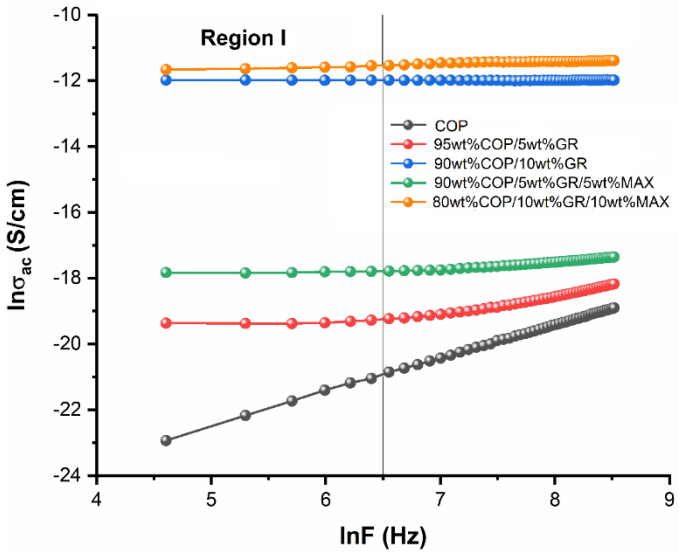

Figure 14. Variation of conductivity of COP and composites with frequency

When the current (I)-voltage (V) graphs of 90wt%COP/10wt%GR and 80wt%COP/10wt% GR/10wt%MAX composites, given in Figure 15, are examined, it is seen that the current increases with increasing voltage and these composites have semiconductor properties.

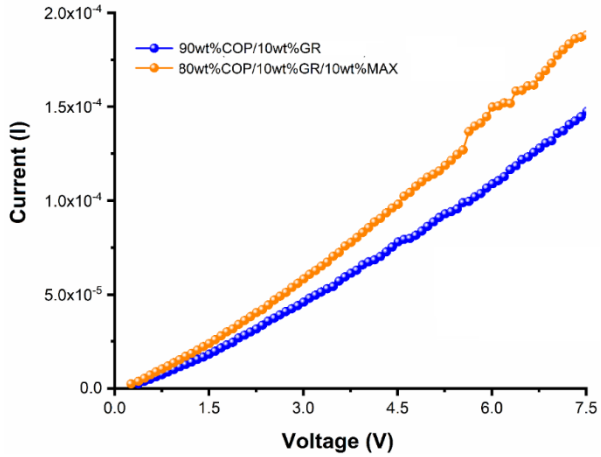

Figure 15. Current (I)-voltage (V) plot of 90wt%COP/10wt%GR and 80wt%COP/10wt%GR/10wt% MAX composites

4. CONCLUSION

In this study, the processability, thermal stability, and dielectric and electrical properties of the COP copolymer and its composites doped with different weight ratios of GR and/or MAX phase (Ti_3AlC_2) were investigated. With the synthesized copolymer, the Tg value, which limits the processability of P(NVC), decreased from 227 °C to 101.74 °C and increased by approximately 2 °C in the composites. However, the results of thermogravimetric analysis revealed that in 10wt%GR and 10wt%GR/10wt%MAX-filled copolymer composites, GR and MAX limited thermal diffusion, thereby increasing the thermal stability of the composites compared to the polymer. This increase in thermal stability may allow the composites to be used at high temperatures or in applications requiring thermal insulation. The composite with 10wt%GR/10wt%MAX-doped polymer exhibited the highest thermal stability at 401.5 °C. A comparison of the thermal degradation activation energy values of the polymer and the 80wt%COP/10wt%GR/10wt%MAX composite, calculated according to the FWO and KAS methods, showed that GR and MAX had a significant effect on the polymer, accelerating the degradation process and reducing the E_a value of the polymer. The investigated dielectric properties of the copolymer and its composites showed that doping improved the dielectric properties of the polymer. With 10wt%GR doping, the dielectric constant of the polymer increased by a factor of 5.5. These increases were also observed in dielectric loss. As the proportion of graphite and MAX in the composites increased, both the dielectric constant and dielectric loss showed further increases. These enhancements in dielectric properties indicate that the composites are well polarized at low frequencies in the direction of the applied electric field. Among the composites, it was observed that conductivity increased with higher GR and MAX concentrations, with the 90wt%COP/10wt%GR and 80wt%COP/10wt%GR/10wt%MAX composites demonstrating semiconducting properties. As a result, the studied materials could be considered for applications requiring both thermal stability and processability, and given their dielectric-conductivity properties, they hold potential for use as functional components in energy storage devices.

Declaration of Ethical Standards

Authors declare to comply with all ethical guidelines including authorship, citation, data reporting, and publishing original research

Credit Authorship Contribution Statement

E.BARIM: Investigation, Experimental Section, Writing-review and editing, Resources, Supervision
E.GUNDOGDU: Investigation, Experimental Section, Resources.

Declaration of Competing Interest

The authors declare that they have no known competing financial interests or personal relationships that could have appeared to influence the work reported in this paper.

Funding / Acknowledgements

This study was not funded by any institution

Data Availability

The data that support the findings of this study are available from the corresponding author.

REFERENCES

[1] S. Demirezen, M. Ulusoy, H. Durmus, H. Cavusoglu, K. Yılmaz and S. Altındal, “Electrical and

photodetector characteristics of schottky structures interlaid with P (EHA) and P (EHA-co-AA) functional polymers by the iCVD method", *ACS omega*, vol 8, no. 49, pp. 46499-46512, 2023.

[2] K. Demirelli, E. Barım, H. Tuncer, G. Barım and A. M. Abubakar, "Synthesis and characterization of N-(2-acetyl benzofuran-3-yl) methacryl amide and ethyl methacrylate copolymer/graphite oxide composites and study of their kinetic and electrical properties", *Polymer Bulletin*, vol 79, no. 7, pp. 4721-4743, 2022.

[3] G. Barim, C. A. Canbay, O. Karaduman and C. Ahmedova, "Synthesis and electrical, thermal and structural characterization of polyaniline doped with Ho_2S_3-In_2S_3", *Journal of Materials and Electronic Devices*, vol 1, no. 1, pp. 49-54, 2019.

[4] S. M. Mousavi, S. A. Hashemi, M. Y. Kalashgrani, A. Gholami, Y. Mazaheri, M. Riazi, D. Kurniawan, M. Arjmand, O. Madkhali, M. D. Aljabri, M. M. Rahman, and W. H. Chiang, "Bioresource Polymer Composite for Energy Generation and Storage: Developments and Trends", *The Chemical Record*, vol 24, no. 1, pp. e202200266, 2024.

[5] A. M. El-naggar, N. Alhaqbani, A. A. Alsaleh, A. M. Kamal, A. A. Albassam and A. M. Aldhafiri, "Structural, optical characteristics, and Poole–Frenkel emission in PMMA/PVAc/TBAI/milled MWCNTs polymer composites for optoelectronic applications", *Optical and Quantum Electronics*, vol 56, no. 8, pp. 1281, 2024.

[6] B. Ates, S. Koytepe, A. Ulu, C. Gurses and V. K. Thakur, "Chemistry, structures, and advanced applications of nanocomposites from biorenewable resources", *Chemical Reviews*, vol 120, no. 17, pp. 9304-9362, 2020.

[7] N. Karthi, K. Kumaresan, S. Sathish, S. Gokulkumar, L. Prabhu and N. Vigneshkumar, "An overview: Natural fiber reinforced hybrid composites, chemical treatments and application areas", *Materials today: proceedings*, vol 27, no.3, pp. 2828-2834, 2020.

[8] D. G. Atinafu, Y. S. Ok, H. W. Kua and S. Kim, "Thermal properties of composite organic phase change materials (PCMs): A critical review on their engineering chemistry", *Applied thermal engineering*, vol 181, no. Aug., pp. 115960, 2020.

[9] D. Das, P. Gopikrishna, R. Narasimhan, A. Singh, A. Dey, P. K. Iyer, "White polymer light emitting diodes based on PVK: the effect of the electron injection barrier on transport properties, electroluminescence and controlling the electroplex formation", *Physical Chemistry Chemical Physics,* vol 18, no. 48, pp. 33077-33084, 2016.

[10] S. Wang, S. Yang, C. Yang, Z. Li, J. Wang, W. Ge, "Poly (Nvinylcarbazole)(PVK) photoconductivity enhancement induced by doping with CdS nanocrystals through chemical hybridization", *The Journal of Physical Chemistry B*, vol 104, no. 50, pp. 11853-11858, 2000.

[11] J. M. Pearson, *Concise Encyclopaedia of Polymer Science and Engineering*. NY: Wiley Interscience Publications, 1990.

[12] R. C. Penwell, B. N. Ganguly and T. W. Smith, ''Poly (N-vinylcarbazole): A selective review of its polymerization, structure, properties, and electrical characteristics'', *Journal of Polymer Science: Macromolecular Reviews*, vol 13, no. 1, pp. 63-160, 1978.

[13] D. Ghosh, P.S. Sardar, M. Biswas, A. Mondal and N. Mukherjee, ''Dielectric characteristics of poly (N-vinylcarbazole) and its nanocomposites with ZnO and acetylene black'', *Materials Chemistry and Physics*, vol 123, no. 1, pp. 9-12, 2010.

[14] J. M. Pearson and M. Stolka, *Poly(N-vinylcarbazole), (Polymer Monographs).* NY: Gordon and Breach, 1981.

[15] K. Maex, M. R. Baklanov, S. H. Brongersma and Z. S. Yanovitskaya, ''Low dielectric constant materials for microelectronics'', *Journal Applied Physics.* vol 93, no. 11, pp. 8793-8841, 2003.

[16] K. Yang, X. Huang, Y. Huang, L. Xie and P. Jiang, ''Fluoro-polymer@$BaTiO_3$ hybrid nanoparticles prepared via RAFT polymerization: toward ferroelectric polymer nanocomposites with high dielectric constant and low dielectric loss for energy storage application'', *Chemistry of Materials*, vol 25, no. 11, pp. 2327-2338, 2013.

[17] F. Biryan and K. Demirelli, ''Copolymerization of benzyl methacrylate and a methacrylate bearing

benzophenoxy and hydroxyl side groups: Monomer reactivity ratios, thermal studies and dielectric measurements'', *Fibers and Polymers*, vol 18, no. 9, pp. 1629-1637, 2017.

[18] S. Tazuke and S. Okamura, *Encyclopedia of Polymer Science and Technology*. NY: Wiley, 1971.

[19] A. Ryttel, "Thermomechanical and dielectrical properties of alkyl methacrylate with N-vinyl carbazole copolymers", *Journal of Macromolecular Science, Part A*, vol 34, no. 1, pp. 211-219, 1997.

[20] E. Bilbao, M. Laza, J. L. Vilas, M. T. Garay, M. Rodríguez and L. M. León, "Thermal Degradation of Copolymers of N-Vinylcarbazole with Acrylic and Methacrylic Monomers", *Journal of Macromolecular Science, Part A*, vol 43, no. 7, pp. 1029-1041, 2006.

[21] I. Haldar, A. Kundu, M. Biswas, and A. Nayak, "Preparation and evaluation of a poly (N-vinylcarbazole)–Fe_3O_4 (PNVC–Fe_3O_4) nanocomposite", *Materials Chemistry and Physics*, vol 128, no. 1-2, pp. 256-264, 2011.

[22] R. S. Sonone, V. M. Raut and G. H. Murhekar, "Structural and electroluminescence properties of pure PVK and doped TiO_2 polymer thin films", *International Journal of Advanced Research in Chemical Scienceis*, vol 1, no. 1, pp. 87-94, 2014.

[23] M. Goumri, R. Hatel, B. Ratier and M. Baitoul, "Optical and electrical properties of poly (N-vinylcarbazole)/grapheneoxide nanocomposites for organic semiconductor devices", *Applied Physics A*, vol 126, no. 8, pp. 647, 2020.

[24] A. A. Al-Muntaser, E. Banoqitah, M. A. Morsi, A. Y. Madkhli, J. M. Abdulwahed, R. Alwafi, A. F. Al Naim and A. Saeed, "Fabrication and characterizations of nanocomposite flexible films of ZnO and polyvinyl chloride/poly (N-vinyl carbazole) polymers for dielectric capacitors", *Arabian Journal of Chemistry*, vol 16, no. 10, pp. 105171, 2023.

[25] B. Duran and E. Şimşek, "Poly (N-vinyl carbazole)-TiO_2 composite coating for protection of steel", *Journal of Adhesion Science and Technology*, vol 37, no. 20, pp. 2781-2794, 2023.

[26] A. G. Al Lafi, S. Mousa and G. Alssayes, "A description of the physical ageing and annealing processes in poly (N-vinyl carbazole) using differential scanning calorimetry and two-dimensional correlation mapping analysis", *Journal of Thermal Analysis and Calorimetry*, vol 149, no. 17, pp. 9275-9284, 2024.

[27] Y. Mu, J. Fan, B. Chu, S. Zhong and Y. Cheng, "Synthesis of n-vinyl carbazole from acetylene by a continuous high-pressure liquid-phase process with Inherent safety", *Chemical Engineering Journal*, vol 493, no. Aug., pp. 152642, 2024.

[28] C. C. Sorensen, A. Y. Bello and F. A. Leibfarth, "Stereoselective Polymerization of 3, 6-Disubstituted N-Vinylcarbazoles", *ACS Macro Letters*, vol 13, no. 5, pp. 614-620, 2024.

[29] M. Xie, F. Chen, J. Liu, T. Yang, S. Yin, H. Lin, Y. Xue and S. Han, "Synthesis and evaluation of benzyl methacrylate-methacrylate copolymers as pour point depressant in diesel fuel", *Fuel*, vol 255, no. Nov., pp. 115880, 2019.

[30] K. Ueno, "Soft materials based on colloidal self-assembly in ionic liquids", *Polymer Journal*, vol 50, no. 10, pp. 951-958, 2018.

[31] C. Yoon, H. S. Kwon, J. S. Yoo, H. Y. Lee, J. H. Bae and J. H. Choi, "Preparation of thermally stable dyes derived from diketopyrrolopyrrole pigment by polymerisation with polyisocyanate binder", *Coloration Technology*, vol 131, no. 1, pp. 2-8, 2015.

[32] M. Worzakowska, "Starch-g-poly (benzyl methacrylate) copolymers: characterization and thermal properties", *Journal of Thermal Analysis and Calorimetry*, vol 124, no. Feb., pp. 1309-1318, 2016.

[33] K. Demirelli, M. Coskun and E. Kaya, "Polymers based on benzyl methacrylate: Synthesis via atom transfer radical polymerization, characterization, and thermal stabilities", *Journal of Polymer Science Part A: Polymer Chemistry*, vol 42, no. 23, pp. 5964-5973, 2004.

[34] X. Liu, X. Dai, W. Boyko, A. S. Fleischer and G. Feng, "Surfactant-mediated synthesis of monodisperse Poly (benzyl methacrylate)-based copolymer microspheres", *Colloids and Surfaces A: Physicochemical and Engineering Aspects*, vol 633, no. 2, pp. 127870, 2022.

[35] D. D. L. Chung, "Review graphite", *Journal of materials science*, vol 37, no. 8, pp. 1475-1489, 2002.

[36] F. Biryan and K. Demirelli, ''Thermal decomposition, kinetics and electrical measurements of Poly (3-Acetamidopropyl Methacrylate)/graphite composites'', *Ferroelectrics*, vol 550, no. 1, 51-75, 2019.

[37] S. Maletić, N. Jović Orsini, M. Milić, J. Dojčilović and A. Montone, "Dielectric properties of epoxy/graphite flakes composites: Influence of loading and surface treatment", *Journal of Applied Polymer Science*, vol 141, no. 5, pp. e54881, 2024.

[38] C. Tu, F. Zhang, J. Zheng, Y. Zhang, Y. Liang, J. Cao, F. Kong, Y. Yang, N Lin, N. Zhang, X. Chen, F. Wang and W. Zhou, "Interfacial insight into elevated dielectric properties in graphite nanosheets reinforced PVDF composites via engineering TiO_2 shell as an interlayer", *Journal of Polymer Research*, vol 31, no. 2, pp. 31, 2024.

[39] M. W. Barsoum, "The MN+ 1AXN phases: A new class of solids: Thermodynamically stable nanolaminates", *Progress in solid state chemistry*, vol 28, no. 1-4, pp. 201-281, 2000.

[40] M.W. Barsoum, D. Brodkin and T. El-Raghy, "Layered Machinable Ceramics for High Temperature Applications", *Scripta Materialia*, vol 36, no. 5, 1997.

[41] M.W. Barsoum and T. El-Raghy, "The MAX Phases: unique New Carbide and Nitride Materials Ternary ceramics turn out to be surprisingly soft and machinable, yet also heat-tolerant, strong and lightweight", *American Scientist*, vol 89, no. 4, pp. 33443, 2001.

[42] P. Eklund, M. Beckers, U. Jansson, H. Högberg and L. Hultman, "The Mn+ 1AXn phases: materials science and thin-film processing", *Thin Solid Films*, vol 518, no. 8, 1851-1878, 2010.

[43] J. Zhang, K. Chen and X. Sun, MAX phase ceramics/composites with complex shapes, *ACS Applied Materials & Interfaces*, vol 13, no. 4, 5645-5651, 2021.

[44] K. Dash and A. Dash, "In-situ formation of 2D-TiCx in Cu-Ti_2AlC composites: an interface reaction study", *Materials Letters*, vol 284, no. 2, 128935, 2021.

[45] E. Barım, "Synthesis, Characterization, Optical and Thermal Properties of P (NVC-co-BZMA) Copolymer and Its ZnO Composites", *Gazi University Journal of Science Part A: Engineering and Innovation*, vol 9, no. 4, 526-536, 2022.

[46] I. Haldar, A. Kundu, M. Biswas and A. Nayak, "Preparation and evaluation of a poly(N-vinylcarbazole)–Fe_3O_4 (PNVC–Fe_3O_4) nanocomposite", *Materials Chemistry and Physics*, vol 128, no. 1-2, 256-264, 2011.

[47] S. Bashir, M. S. Awan, M. A. Farrukh, R. Naidu, S. A. Khan, N. Rafique, S. Ali, I. Hayat, I. Hussain and M. Z. Khan, "In-vivo (Albino Mice) and in-vitro Assimilation and Toxicity of Zinc Oxide Nanoparticles in Food Materials", *International Journal of Nanomedicine*, vol 17, no. Sep., 4073-4085, 2022.

[48] S. A. El-Khodary, G. M. El-Enany, M. El-Okr and M. Ibrahim, "Preparation and characterization of microwave reduced graphite oxide for high-performance supercapacitors", *Electrochimica Acta*, vol 150, no. Dec., 269-278, 2014.

[49] K. M. Rehan, B. Anbarasu, P. M. Ashfaque, S. M. Safiullah and K. A. Basha, ''Synthesis and characterization of poly (vinyl carbazole-co-ethoxy ethyl methacrylate) and its nanocomposites'', *Materials Today: Proceedings*, vol 50, no. 3, 325-330, 2022.

[50] K. Demirelli, A. M. Abubakar, A. A. Ahmad and E. Bagcı, "The effect of end group and graphene on dielectric properties and thermal degradation of poly(benzyl methacrylate) prepared by ATRP method", *Polymer Bulletin*, vol 80, no. 1, pp. 279-307, 2022.

[51] M. Akshay, S. Jyothilakshmi, Y. S. Lee, V. Aravindan, ''CuS modified graphite from spent Li-ion batteries towards building high energy Na-ion capacitors via solvent-co-intercalation process'', *Chemical Engineering Journal*, vol 498, no. 1, 155462, 2024.

[52] M. Mahmood, A. Rasheed, I. Ayman, T. Rasheed, S. Munir, S. Ajmal, P. O. Agboola, M. F. Warsi, and M. Shahid, "Synthesis of Ultrathin MnO_2 Nanowire-Intercalated 2D-MXenes for High-Performance Hybrid Supercapacitors", *Energy & Fuels*, vol 35, no. 4, 3469-3478, 2021.

[53] A. Syuy, D. Shtarev, A. Lembikov, M. Gurin, R. Kevorkyants, G. Tselikov, A. Arsenin and V. Volkov, ''Effective Method for the Determination of the Unit Cell Parameters of New MXenes. Materials'', *Materials*, vol 15, no. 24, 8798, 2022.

[54] E. Marimuthu and V. Murugesan, ''Influence of ultrasound on multi-site phase transfer catalyzed polymerization of N-vinyl carbazole in two phase system'', *SN Applied Sciences*, vol 1, no. 6, 638, 2019.

[55] Z. Mao and J. Zhang, "Toughening effect of CPE on ASA/SAN binary blends at different temperatures", *Journal of Applied Polymer Science*, vol 133, no. 20, pp. 43353, 2016.

[56] D. Kapusuz, "Production and structural analysis of Ti_3AlC_2/Ti_3C_2 incorporated epoxy composites", *Konya Journal of Engineering Sciences*, vol 7, no. 3, pp. 632-644, 2019.

[57] M. Coskun, G. Barim and K. Demirelli, "Thermal stabilities of poly(n-acryloyl-n'-methylpiperazine), its blends with poly(methyl methacrylate), and poly(n-acryloyl-n'-methylpiperazine-co-methyl methacrylate)", *Journal of Macromolecular Science, Part A*, vol 43, no. 1, 83-93, 2006.

[58] D. Liu, L. Hentschel, G. Lin, C. Kukla, S. Schuschnigg, N. Ma, C. Wallis, V. Momeni, M. Kitzmantel and G. Sui, "Multifunctional Ti_3AlC_2-Based Composites via Fused Filament Fabrication and 3D Printing Technology", *Journal of Materials Engineering and Performance*, vol 32, no. 20, pp. 9174-9181, 2023.

[59] S. Vyazovkin, A. K. Burnham, J. M. Criado, L.A. Pérez-Maqueda, C. Popescu and N. Sbirrazzuoli, "ICTAC Kinetics Committee recommendations for performing kinetic computations on thermal analysis data", *Thermochim Acta,* vol 520, no. 1, 1-19, 2011.

[60] D. N. Waters and J. L. Paddy, "Equations for isothermal differential scanning calorimetric curves", *Analytical Chemistry*, vol 60, no. 1, pp. 53-57, 1988.

[61] D. S. Achilias, E. Panayotidou and I. Zuburtikudis, "Thermal degradation kinetics and isoconversional analysis of biodegradable poly (3-hydroxybutyrate)/ organomodified montmorillonite nanocomposites", *Thermochimica Acta*, vol 514, no. 1, pp. 58-66, 2011.

[62] S. Ceylan and Y. Topçu, "Pyrolysis kinetics of hazelnut husk using thermogravimetric analysis", *Bioresource Technology*, vol 156, no. 182, 182-188, 2014.

[63] S. Bano, N. Ramzan, T. Iqbal, H. Mahmood and F. Saeed, "Study of thermal degradation behavior and kinetics of ABS/PC blend", *Polish Journal of Chemical Technology*, vol 22, no. 3, pp. 64-69, 2020.

[64] S. Vyazovkin, K. Chrissafis, M. L. Di Lorenzo, N. Koga, M. Pijolat, B. Roduit, N. Sbirrazzuoli and J. J. Sunol, "ICTAC Kinetics Committee recommendations for collecting experimental thermal analysis data for kinetic computations", *Thermochimica Acta*, vol 590, no. Aug., pp. 1-23, 2014.

[65] J. H. Flynn and L. A. Wall, "General treatment of the thermogravimetry of polymers", *Journal of Research of the National Bureau of Standards*, vol 70, no. A6, pp. 487-523, 1966.

[66] T. Ozawa, "A new method of analyzing thermogravimetric data", *Bulletin of the Chemical Society of Japan*, vol 38, no. 11, pp. 1881-1886, 1965.

[67] H. E. Kissinger, "Reaction Kinetics in Differential Thermal Analysis", *Analytical Chemistry*, vol 29, no. 11, pp. 1702-1706, 1957.

[68] K. Chrissafis, "Kinetics of thermal degradation of polymers: complementary use of isoconversional and model-fitting methods", *Journal of Thermal Analysis and Calorimetry*. Vol 95, no. 1, pp. 273-283, 2008.

[69] P. Seven, , M. Coskun and K. Demirelli, "Synthesis and characterization of two-armed graft copolymers prepared with acrylate and methacrylate using atom transfer radical polymerization", *Reactive and Functional Polymers*, vol 68, no. 5, pp. 922–930, 2008.

[70] S. Rajendran and M. Ramesh Prabhu, "Effect of different plasticizer on structural and electrical properties of PEMA-based polymer electrolytes", *Journal of Applied Electrochemistry*, vol 40, no. 2, pp. 327-332, 2010.

[71] K. W. Wagner, "Erklärung der dielektrischen Nachwirkungsvorgänge auf Grund Maxwellscher Vorstellungen" *Archiv für Elektrotechnik*, vol 2, no. 9, 371-387, 1914.

[72] L. K. H. Van Beek, "Progress in Dielectrics", J. B. Birks ed., Heywood, London, vol 7, no. 71, pp. 69-113, 1967.

[73] W. J. Wang, C. W. Li and K. P. Chen, "Electrical, dielectric and mechanical properties of a novel

Ti_3AlC_2/epoxy resin conductive composites", *Materials Letters*, vol 110, no. Nov., pp. 61-64, 2013.

[74] S. Ningaraju, , N. H. Vinayakaprasanna, , A. P. Gnana Prakash and H. B. Ravikumar, "Free volume dependence on electrical properties of Poly (styrene co-acrylonitrile)/Nickel oxide polymer nanocomposites", *Chemical Physics Letters*, vol 698, no. Apr., pp. 24-35, 2018.

[75] E. Jayamani, T. C. Peng, M. K. B. Bakri and A. Kakar, "Comparative Analysis on Dielectric Properties of Polymer Composites Reinforced With Synthetic and Natural Fibers", *Journal of Vinyl & Additive Technology,* vol 24, no. S1, pp. E201-E216, 2018.

[76] H. Li, Z. Chen, L. Liu, J. Chen, M. Jiang and C. Xiong, "Poly(vinylpyrrolidone)-coated graphene/poly(vinylidene fluoride) composite films with high dielectric permittivity and low loss", *Composites Science and Technology*, vol 121, no. Dec., pp. 49-55, 2015.